



HAL
open science

High peak power pulsed fiber laser with high efficiency based on an ytterbium doped powder sinter fiber

Maxime Chenou, Alain Mugnier, Paul Mouchel, Céline Canal, Guillaume Canat, Romain Dauliat, Baptiste Leconte, Raphaël Jamier, Philippe Roy

► To cite this version:

Maxime Chenou, Alain Mugnier, Paul Mouchel, Céline Canal, Guillaume Canat, et al.. High peak power pulsed fiber laser with high efficiency based on an ytterbium doped powder sinter fiber. *Fiber Lasers XVII: Technology and Systems*, Feb 2020, San Francisco, United States. pp.71, 10.1117/12.2546351 . hal-02524364

HAL Id: hal-02524364

<https://hal.science/hal-02524364>

Submitted on 14 Dec 2020

HAL is a multi-disciplinary open access archive for the deposit and dissemination of scientific research documents, whether they are published or not. The documents may come from teaching and research institutions in France or abroad, or from public or private research centers.

L'archive ouverte pluridisciplinaire **HAL**, est destinée au dépôt et à la diffusion de documents scientifiques de niveau recherche, publiés ou non, émanant des établissements d'enseignement et de recherche français ou étrangers, des laboratoires publics ou privés.

High peak power pulsed fiber laser with high efficiency based on an ytterbium doped powder sinter fiber

M. Chenou¹, A. Mugnier¹, P. Mouchel¹, C. Canal¹, G. Canat¹, R. Dauliat²,
B. Leconte², R. Jamier², P. Roy²

¹ Keopsys Industries, Lumibird, 2 Rue Paul Sabatier, 22300 Lannion, France

² Xlim, Photonics Department, UMR CNRS 6172, 123 Avenue Albert Thomas,
87060 Limoges, France

ABSTRACT

High power diffraction-limited 1064 nm fiber lasers operating in the nanosecond regime can be used for long-range LIDAR and micromachining applications. Peak power is limited by non-linearities, there is therefore an interest to develop fibers exhibiting a very large mode field effective area. New fibers are being developed in the frame of the 4F consortium ("French laser Fibers for Factories of the Future") to fulfill this need.

We report on results obtained with a new 39 μm core diameter polarization maintaining ytterbium doped fiber that has been manufactured using the powder sintering technology. It features a large cladding absorption close to 20 dB/m at 976 nm (small signal) and a mode field diameter close to 32 μm .

We built a pulsed MOPA. The preamplifier generates 2.5 ns pulses at 1064 nm with 8.5 W average power at 1 MHz pulse repetition frequency. The power amplifier is based on the 39 μm core fiber with 215/230 μm hexagonal cladding counter-pumped at 976 nm. It features 72 % slope efficiency delivering 72.2 W average power at a pulse repetition rate of 1 MHz. An end-cap was spliced to the fiber output to increase the damage threshold. At 100 kHz a peak power of 351 kW was measured for an average power of 59.9 W. The efficiency is then 70 %. This good efficiency shows that the composition was well optimized.

We also studied the influence of the bending radius on the slope efficiency. We do not observe any slope efficiency reduction down to 25 cm bending diameter. It decreased to 68 % for the 20 cm bending diameter. The laser shows a quasi-singlemode output beam with a good quality factor M^2 of 1.2.

Keywords: large mode area fiber; ytterbium fiber laser

1. INTRODUCTION

High power diffraction-limited 1064 nm fiber lasers operating in the nanosecond regime can be used for long range lidar and micromachining applications. Peak power is limited by non-linearities and there is an interest to develop fibers with very large mode field effective area. Rod types (LPF or rod-type fiber) offer very large effective area but they lack flexibility for easy integration. The main problems of further energy scaling with bendable fibers are technical difficulties to preserve singlemodedness, that is to say on controlling numerical apertures smaller than 0.04, which is currently the state-of-the-art of modern MCVD technology. To alleviate this issue, fiber manufacturers produce filamented-core materials by using a multiple stack-and-draw approach which is time-consuming and cost ineffective. As an alternative, a recently developed synthesis technique based on the powder technology and known as Repusil, has shown excellent performances for the fabrication of high-power fiber lasers [1] and for the enhancement of the control over the refractive index value, homogeneity and reproducibility [2]. Recently, the Leibniz Institute of Photonic Technology team demonstrated 375 kW peak power with M^2 between 1.3 and 1.7 using a tapered rod obtained from REPUSIL technology [3]. However, the spectrum showed substantial Raman scattering. New fibers are being developed in the frame of the 4F consortium ("French laser Fibers for Factories of the Future") to fill this need. We have developed a 39 μm core diameter polarization maintaining ytterbium doped fiber that has been prepared using the powder sintering technology and used it to demonstrate pulse amplification up to 351 kW peak power without observation of Raman scattering.

2. FIBER CONCEPT AND MANUFACTURING

Preparing step-index LMA fibers is a challenging task, since it requires a fine control of the numerical aperture (NA) between the core and the cladding material. Until recently, most traditional synthesis approaches such as MCVD hardly allowed the fabrication of a step-index fiber whose the NA is smaller than 0.04 ($\Delta n = 5 \cdot 10^{-4}$), restricting the core size to about 15 μm at 1 μm operating wavelength or requiring the assistance of the bending to ensure singlemodedness [4]. However, some recent work demonstrated a singlemode behavior with a NA as low as 0.025 in a rod-type fibre [5]. In this publication, authors relied on the powder sintering approach [6] for an accurate and fine control of the refractive index contrast. The cross section of the fabricated low-NA 39- μm core PM fiber is depicted below.

First, the 39 μm fiber core material was doped with 1000 ppm.mol Yb-ions and codoped with Al_2O_3 . This resulted in a NA of 0.1 regarding the F300 grade pure silica. Then, to ensure a singlemode operation, a pedestal material made of Al_2O_3 -doped silica was synthesized, reducing the core NA down to 0.042. Two boron-doped rods have also been implemented for ensuring a PM feature. Finally, the implementation of an outer silica jacket and a low-index polymer yields in a triple clad geometry. The 210*235 μm pump cladding has been chosen hexagonal to provide an efficient cladding pump light absorption, close to 20 dB/m at 976 nm (small signal).

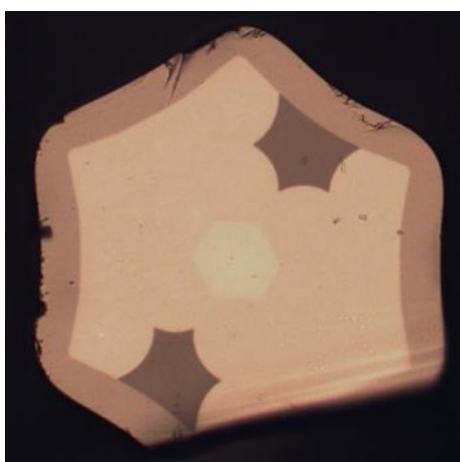


Fig.1 – Cross-sectional microscope image of the 39 μm core PM Yb-doped fiber used in this work

3. EXPERIMENTAL RESULTS

3.1 Experimental setup

In order to assess this fiber performances, we built a MOPA architecture represented on Fig. 2. The seeder is a pulsed DFB laser diode operating at 1064 nm. It is preamplified by a Keopsys ytterbium PM fiber amplifier, with 2.5 ns pulse duration and an adjustable pulse repetition frequency (PRF) in the range of 100 Hz to 1 MHz. It is terminated with a high-power fiber collimator (20 /125 μm 0.08 NA), protecting it from optical returns. The amplified beam is linearly polarized, with a polarization extinction ratio (PER) around 28 dB. The average output power was measured just after the collimator ranging from 1 to 10 W depending on the PRF.

The 0.7 mm diameter collimated beam then passed through a 10 nm width bandpass filter, used to eliminate any noise such as amplified spontaneous emission (ASE) or stimulated Raman scattering (SRS) generated in the seeder. This filter was also chosen as a second protection from possible optical returns. It is then reflected by two short-pass dichroic mirrors and coupled into the LMA ytterbium doped fiber with an $f = 15$ mm aspherical lens.

The input fiber end was carefully prepared and cleaved at a 3° angle then attached to a 3-axis translation stage. This scheme allows to precisely maximize the injected power by tuning the dichroic mirrors, lens and fiber positions.

The 2.7 m long fiber was placed on an airflow cooled heatsink and coiled around given diameter cylinders ($D = 20, 25$ and 30 cm). On each end, almost 20 cm of fiber were set straight on the heatsink. The end face of the fiber was also carefully prepared and spliced to a homemade packaged silica endcap with 8° face angle. The role of this endcap was to distribute the high-power density on a wider surface to increase power damage threshold and reduce return loss.

The fiber was counter pumped by a wavelength-stabilized fiber-coupled ($105 / 125 \mu\text{m}$ 0.22 NA) laser diode providing up to 140 W at 976 nm. The pump beam was coupled into the fiber by two aspherical lenses $f = 20$ and 15 mm through a 3rd short pass dichroic mirror. The non-absorbed pump power was transmitted through the 2nd dichroic to a powermeter.

The amplified signal was reflected by the 3rd dichroic mirror to a measurement stage using mirrors and wedged plates to collect attenuated light upon varied equipment such as a powermeter a photodiode, an optical spectrum analyzer (OSA) and a CCD camera.

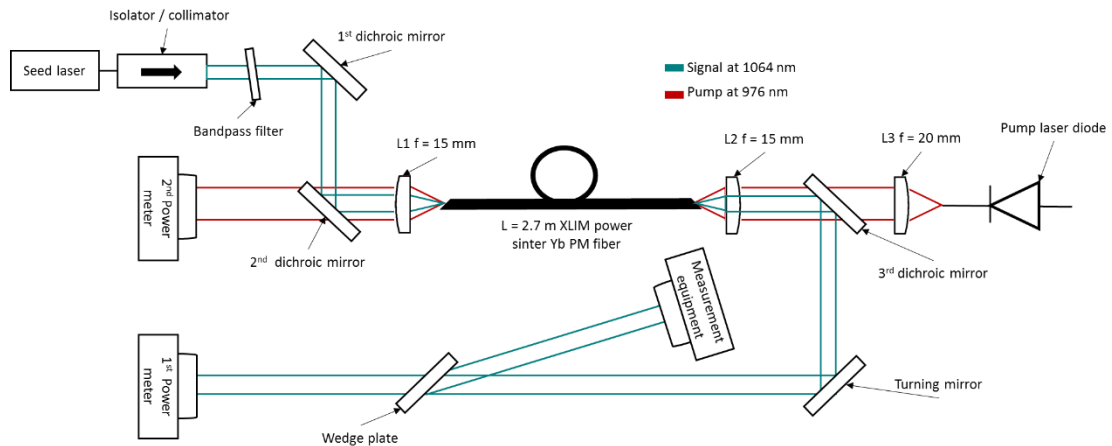


Fig.2 – Experimental setup

3.2 Results:

We performed various amplification experiments to quantify the fiber's performances. At first, we set a 1 MHz PRF resulting in a launched average power of 8.5 W. We measured that 89 % of it were actually coupled to the fiber which was coiled on a $D = 25$ cm diameter.

In these conditions we achieved up to 72.2 W average power with a launched pump power of 105 W. The estimated peak power was around 28 kW. The 2nd powermeter allowed us to retrieve the amount of absorbed pump power resulting in a direct efficiency (signal power versus absorbed pump power) of 71.9 % as plotted in Fig. 3.

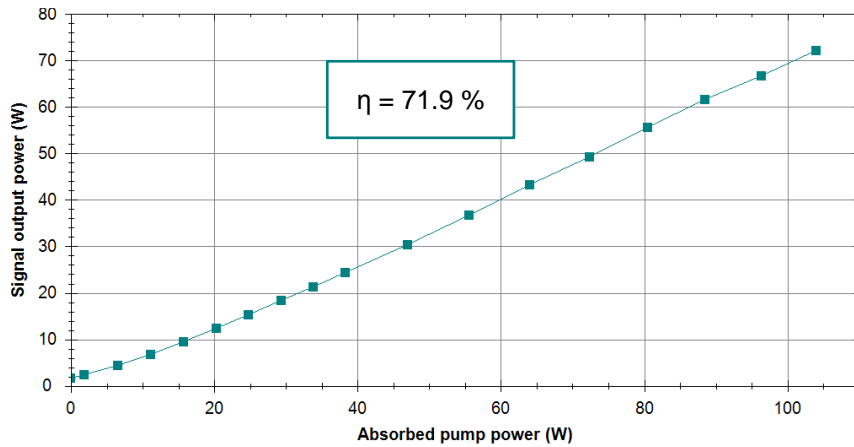


Fig.3 – Evolution of output average power versus absorbed pump power at PRF =1 MHz

We investigated the influence of fiber bending along different diameters on the direct efficiency value. We kept the same settings as for Fig.3 but changed the bending diameter to $D_0= 20$ cm and $D_1= 30$ cm. We obtained pump efficiencies of respectively $\eta_0 = 67.9\%$ and $\eta_1 = 71.2\%$ as showed in Fig. 4.

These results show that we could use the fiber down to a minimum of 20 cm diameter while reducing it further would probably reduce the efficiency as the bending loss on the signal gets stronger.

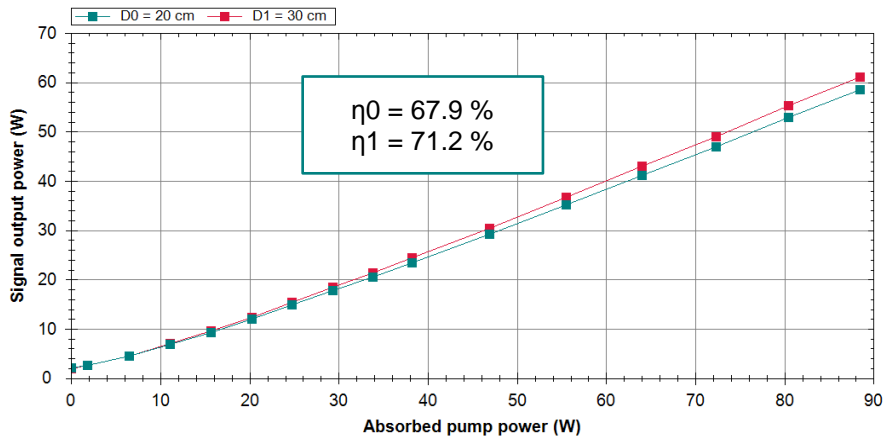


Fig.4 – Influence of bending radius on direct efficiency at PRF =1 MHz

We also investigated the amplifier performances relative to the polarization quality by adding a half-wave plate before L1 and a polarization beam splitter cube before the 1st power meter. We obtained a PER of 11.6 dB in this case while previous experiments with a continuous wave seeder shown up to 15 dB extinction. The measurement difference might result from light trapped in the fiber's pedestal affecting the extinction or from other experiment bias.

Afterwards, the peak power capability of the fiber was investigated by reducing the PRF to 100 kHz. This reduced the launched seed power to 2.5 W and the injected power to 2.2 W. In this configuration the average power reached up to 59.9 W for 93.5 W of pump power with a direct efficiency of 69.9 % as plotted in Fig. 5.

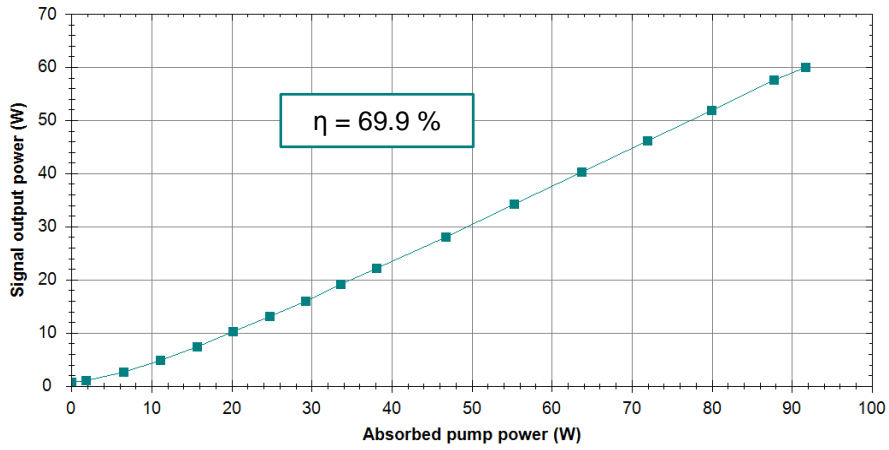


Fig.5 – Evolution of output average power versus absorbed pump power at PRF =100 kHz

For the energy measurement, we calibrated our photodiode and oscilloscope system at an high PRF, free of any noise ASE or nonlinear effects at a settled 1 W average output power allowing an easy calculation of the conversion factor between V read on the oscilloscope and the corresponding W pulse power level. We then acquired the maximum voltage and integrated the pulses shapes to get a value in V.s then converted to μJ using the conversion factor. In conclusion, we obtained up to 351 kW for the highest peak power and 598 μJ of energy.

The optical spectra at maximum achieved power setpoints are plotted in the Fig. 6 below for both studied PRF. The 351 kW peak power curve, at PRF = 100 kHz, displays a non linear broadening around the center wavelength but shows neither SRS around 1120 nm nor ASE around 1030 nm. We had preliminarily verified our setup transmission at those wavelengths meaning the fiber has a rather high SRS threshold.

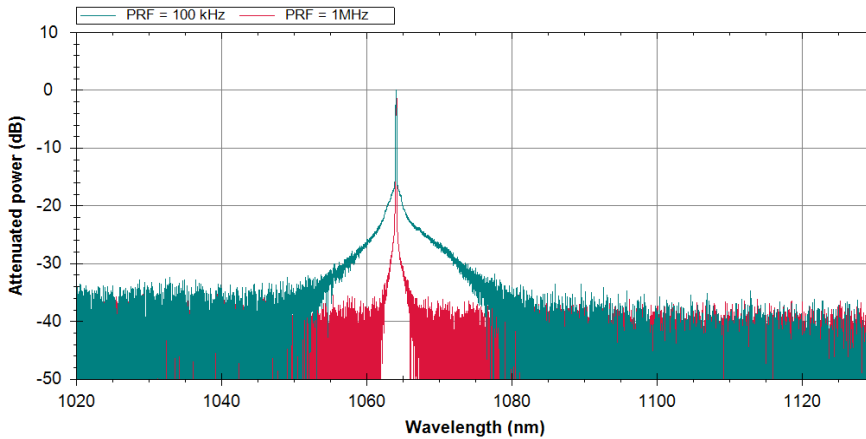


Fig.6 – Output spectrum at PRF =1MHz and 100 kHz

The beam intensity profile was measured using a CCD camera resulting in the Fig. 7. It follows a quasi-gaussian distribution but shows little power remaining in the cladding. The profile is stable over time and the fundamental mode is favored by the amplification, therefore the amount of energy brought by high order modes is fairly low and the fiber exhibit quasi singlemode operation as expected from its design. We obtained an average M^2 of 1.2 among both axes and a mode field diameter of 32 μm .

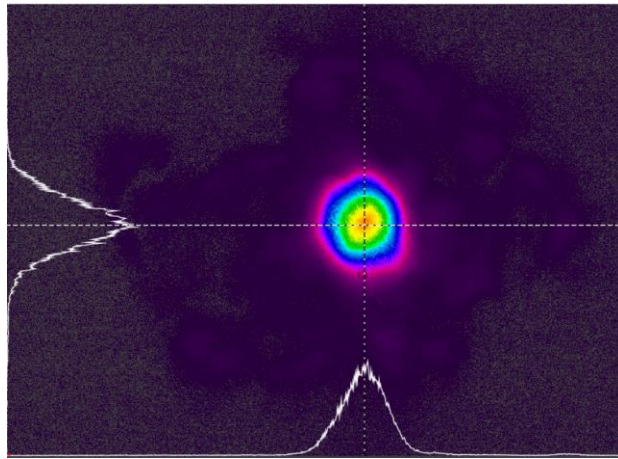


Fig.7 – Beam intensity profile at PRF = 1MHz and 72.2 W average power

4. MODELLING RESULTS

4.1 Modal properties

In order to compute the effective area, we used a vectorial finite element model (COMSOL). The core was modelled as an equivalent step index circular core with stress applying parts on each side. The whole fiber is surrounded by a perfectly matched layer. The fundamental mode is shown on Fig. 8. Using this model, we can compute the fundamental mode effective area as a function of the effective bending radius. We can observe on Fig. 9 the well-known reduction of the effective area for small bending radius from $700\mu\text{m}^2$ to $500\mu\text{m}^2$. We chose to use the fiber with about 12.5 cm bending radius corresponding to an effective bending radius of 16 cm. For this radius, the fundamental mode loss is 0.01 dB/m (cf. Fig. 10).

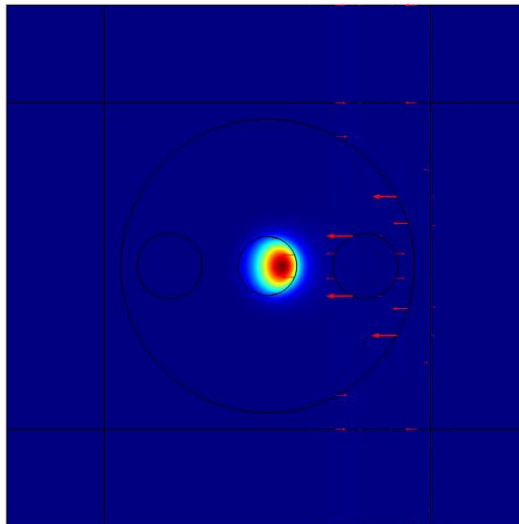


Fig.8 – Fiber modelling and fundamental mode at 12.5 cm bending radius

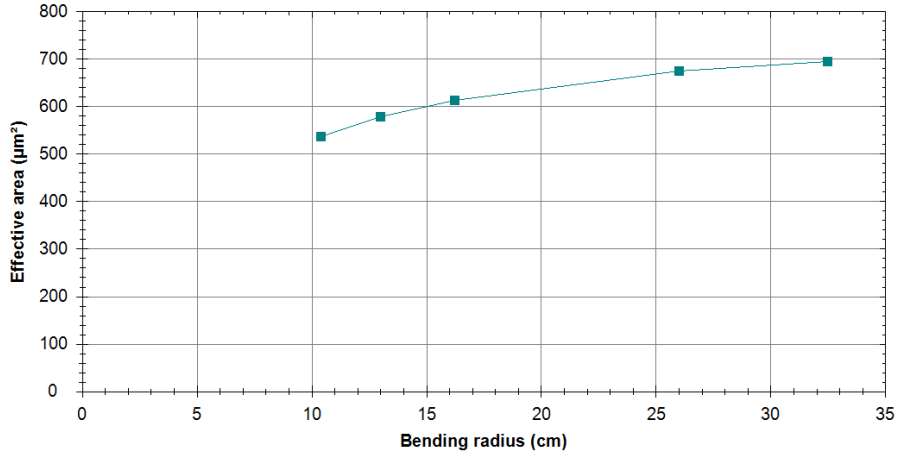


Fig.9 – Modeling results of the dependence of effective area with bending radius

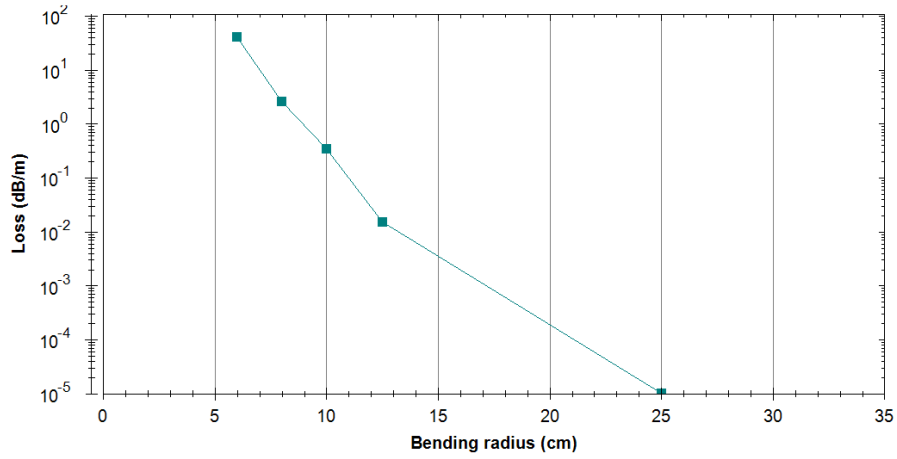


Fig.10 – Variation of propagation losses of the fundamental mode with the bending radius

For the configurations of Fig.5, the output power computed using these models for 90 W pump power are 64 W and 66 W for 20 cm and 30 cm bending diameter respectively when the power lost by bending loss is considered guided by the inner cladding. These values are within 5% of the measurements and the power decrease is 3% as for the experimental values.

4.2 Raman threshold calculation

We used a dynamic model to compute the power distribution along the amplifier at each pulse start. From this calculation we found the effective length $L_{eff} \sim 0.25$ m. Let us define the Raman gain amplifier coefficient X for an amplifier with output power P , Raman gain value g_R , effective area A_{eff} by

$$X = \frac{P g_R L_{eff}}{A_{eff}} \quad (1)$$

Let us define the ratio β between the Stokes Raman power and the signal power. Then we can write from Smith work [7] following Jauregi approach [8]:

$$\frac{\sqrt{\pi}}{2} h\nu_s \Delta\nu \frac{e^X}{X^{1/2}} G_A = \beta P \quad (2)$$

To a good approximation for $P \sim 300$ kW

$$X = 25.4 - \ln G_A + \ln \beta \quad (3)$$

From the previous calculations $L_{\text{eff}}=0.25$ m, $A_{\text{eff}}=577 \mu\text{m}^2$, G_A the gain of the fiber amplifier at 1200 nm the Stokes wavelength (here $G_A=3.5$). Moreover, we assume $\beta \sim 10^{-3}$ corresponding to the spectrum analyzer dynamics and $g_R=10^{-13}$ m/W. From (3) we finally get an estimation of the peak power to detect the Stokes power 420 kW. This is larger than our current peak power confirming that we cannot observe the Stokes peak.

5. CONCLUSION

We have demonstrated generation of 351 kW peak power at 100 kHz pulse repetition frequency using a powder sinter ytterbium doped fiber with 39 μm core size and measured 32 μm MFD. At 1MHz a maximum average power of 72.2 W with 72% efficiency was obtained. The beam quality is excellent with $M^2 \sim 1.2$. Modelling shows that the results are in good agreement with the expectations and that Raman scattering should be observed at 420 kW.

All fiber configuration is currently in development to propose a high-power compact and efficient laser.

ACKNOWLEDGEMENT

Authors thank their collaborators from the Leibniz Institute of Photonics Technology for their advice and scientific guidance in the synthesis of the doped silica materials.

This work was partially funded by Banque Publique d'Investissement in the frame of 4F project. Authors thank BPI and all the partners of project 4F.

REFERENCES

- [1] M. Leich, F. Just, A. Langner, M. Such, G. Schötz, T. Eschrich, S. Grimm, "Highly efficient Yb-doped silica fibers prepared by powder sinter technology," *Opt. Lett.*, vol. 36, no. 9, pp. 1557–9, 2011.
- [2] A. Langner, G. Schötz, M. Such, V. Reichel, S. Grimm, and J. Kirchhof, "A new material for high power laser fibers," *Proc. SPIE*, vol. 6873, pp. 687311–1, 2008.
- [3] Y. Zhu, M. Leich, M. Lorenz, T. Eschrich, C. Aichele, J. Kobelke, H. Bartelt, M. Jäger, "Yb-doped large mode area fiber for beam quality improvement using local adiabatic tapers with reduced dopant diffusion," *Opt. Express*, vol. 26, no. 13, pp. 17034–17043, 2018.
- [4] D. Jain, Y. Jung, P. Barua, S. Alam, and J. K. Sahu, "Demonstration of ultra-low NA rare-earth doped step index fiber for applications in high power fiber lasers," *Opt. Express*, vol. 23, no. 6, pp. 5200–5203, 2015.
- [5] V. Petit, R. P. Tumminelli, J. D. Minelly, and V. Khitrov, "Extremely low NA Yb doped preforms (<0.03) fabricated by MCVD," *CLEO 2016*, vol. 9728, no. Fig. 1, pp. 97282R-97282R-7, 2016.
- [6] R. Dauliat, A. Benoît, D. Darwich, R. Jamier, J. Kobelke, S. Grimm, K. Schuster, P. Roy, "Demonstration of a Homogeneous Yb-Doped Core Fully-Aperiodic Large-Pitch-Fiber Laser," *Appl. Opt.*, vol. 55, no. 23, pp. 6229–6235, 2016.
- [7] R.G. Smith, "Optical power handling capacity of low loss optical fibers as determined by stimulated Raman and Brillouin scattering," *Appl. Opt.* 11, 2489-2494 (1972)
- [8] C. Jauregui, J. Limpert, A. Tünnermann, "On the Raman threshold of passive large mode area fibers," *Proc. SPIE 7914, Fiber Lasers VIII: Technology, Systems, and Applications*, 791408 (10 February 2011)

